THE JOURNAL OF BIOLOGICAL CHEMISTRY VOL. 285, NO. 9, pp. 6434–6442, February 26, 2010

Zn^{2+} Activates Large Conductance Ca^{2+}-activated K^+ Channel via an Intracellular Domain*[S]

Received for publication, September 23, 2009, and in revised form, December 22, 2009 Published, JBC Papers in Press, December 26, 2009, DOI 10.1074/jbc.M109.069211

Shangwei Hou[‡1], Leif E. Vigeland[§], Guangping Zhang[‡¶2], Rong Xu[‡], Min Li[‖], Stefan H. Heinemann[**], and Toshinori Hoshi[‡]

*From the [‡]Department of Physiology and [§]Neuroscience Graduate Group, University of Pennsylvania, Philadelphia, Pennsylvania 19104, the [¶]Department of Neurobiology, Pharmacology and Physiology, The University of Chicago, Chicago, Illinois 60637, the [‖]Department of Neuroscience and High Throughput Biology Center, The Johns Hopkins University School of Medicine, Baltimore, Maryland 21205, and the **Center for Molecular Biomedicine, Department of Biophysics, Friedrich Schiller University of Jena, Hans-Knöll-Strasse 2, D-07745 Jena, Germany*

Zinc is an essential trace element and plays crucial roles in normal development, often as an integral structural component of transcription factors and enzymes. Recent evidence suggests that intracellular Zn^{2+} functions as a signaling molecule, mediating a variety of important physiological phenomena. However, the immediate effectors of intracellular Zn^{2+} signaling are not well known. We show here that intracellular Zn^{2+} potently and reversibly activates large-conductance voltage- and Ca^{2+}-activated Slo1 K^+ (BK) channels. The full effect of Zn^{2+} requires His^{365} in the RCK1 (regulator of conductance for K^+) domain of the channel. Furthermore, mutation of two nearby acidic residues, Asp^{367} and Glu^{399}, also reduced activation of the channel by Zn^{2+}, suggesting a possible structural arrangement for Zn^{2+} binding by the aforementioned residues. Extracellular Zn^{2+} activated Slo1 BK channels when coexpressed with Zn^{2+}-permeable TRPM7 (transient receptor potential melastatin 7) channels. The results thus demonstrate that Slo1 BK channels represent a positive and direct effector of Zn^{2+} signaling and may participate in sculpting cellular response to an increase in intracellular Zn^{2+} concentration.

Zinc is the second most abundant transition metal in the human body, playing a pivotal role in the normal development and growth. The utmost importance of zinc is evidenced by the diverse array of symptoms that could result from a chronic dietary deficiency of zinc (1). Biochemically, zinc serves as an essential structural and a catalytic component in many metalloproteins (2), in which the metal is typically coordinated by four or five ligands (3). Multiple zinc coordination geometries are known, but histidine and cysteine typically act as essential ligands (4).

In addition to its role as an integral structural and catalytic factor, Zn^{2+} is increasingly recognized as a potential intracellular signaling molecule, similar to Ca^{2+} (5, 6). Like intracellular Ca^{2+}, intracellular Zn^{2+} is normally kept to a very low concentration, from pM to nM (5). Although measurements of free intracellular Zn^{2+} concentrations ($[Zn^{2+}]_i$) in living cells remain challenging, studies do suggest that $[Zn^{2+}]_i$ may significantly increase under some conditions. For example, a robust release of Zn^{2+} from the endoplasmic reticulum, termed "zinc wave," has been observed in response to extracellular stimuli, further suggesting that Zn^{2+} may act as an intracellular second messenger (7). In addition, local $[Zn^{2+}]_i$ may be significantly higher near Zn^{2+}-permeable channels (5, 8), analogous to the well known micro- and nano-domains of intracellular Ca^{2+} (9). Moreover, $[Zn^{2+}]_i$ may increase concomitantly with $[Ca^{2+}]_i$ under pathological conditions such as ischemia/hypoxia (5, 6, 10, 11), in which intracellular Ca^{2+} overload is suspected to contribute to cell death in these conditions (12). However, whether such increases in $[Zn^{2+}]_i$ contribute to the deleterious effect or play a compensatory cell-protective effect is not clear (5, 11, 13–16).

Large-conductance voltage- and Ca^{2+}-activated K^+ (BK_{Ca}, Slo1 BK or $K_{Ca}1.1$) channels are distinguished by their allosteric activation by voltage and intracellular Ca^{2+} (17–19). Like other voltage-gated K^+ channels, a BK channel complex includes four pore-forming α (Slo1) subunits, each of which contains a voltage sensor domain (S1–S4) and one-fourth of the ion conduction pore (S5–S6) (20). In addition, each Slo1 subunit possesses the transmembrane segment S0 (21) and a large cytoplasmic area harboring two homologous domains termed "regulators of conductance of potassium" (RCK1 and RCK2) essential for activation by Ca^{2+} for the channel (22, 23). Functionally, BK channels participate in many crucial physiological phenomena including vasoregulation, synaptic transmission, and hormone secretion mainly by affecting membrane excitability (17). In addition, as a feedback controller of intracellular Ca^{2+}, BK channel activation has been demonstrated to have a potent cell protection effect by limiting the influx of Ca^{2+} during hypoxia/ischemia (24, 25).

The concomitant increases in $[Zn^{2+}]_i$ and $[Ca^{2+}]_i$ in ischemia/hypoxia and the cytoprotective role of the BK channel under the pathological conditions prompted us to examine whether Zn^{2+} is also a physiological activator of the channel. The Slo1 protein indeed contains multiple putative Zn^{2+}-binding amino acid sequences such as H*XXX*H (*X* represents any

* This work was supported in part by National Institutes of Health Grants GM057654 (to T. H.), MH084691 (to M. L.), and GM078579 (to M. L. and T. H.). This work was also supported by Deutsche Forschungsgemeinschaft (HE2993/8).

[S] The on-line version of this article (available at http://www.jbc.org) contains supplemental Fig. S1.

[1] To whom correspondence should be addressed: University of Pennsylvania, 3700 Hamilton Walk, Philadelphia, PA 19104. Fax: 215-573-5851; E-mail: shangwei@mail.med.upenn.edu.

[2] Present address: Dept. of Neurobiology, Pharmacology and Physiology, The University of Chicago, Chicago, IL 60637.

amino acid) identified in other metal-binding proteins including S100 proteins, the largest subgroup of the EF-hand Ca^{2+}-binding protein family (26–28). Our excised patch clamp measurements from heterologously expressed human Slo1 (hSlo1)[3] BK channels revealed that intracellular Zn^{2+} robustly activates the channel and that mutation of one histidine residue in the RCK1 domain fully abolished the stimulatory effect of Zn^{2+}. Our results therefore suggest that Slo1 coordinates Zn^{2+} using amino acid ligands in the RCK1 domain and that the Slo1 BK channel is a positive effector of intracellular Zn^{2+} signaling.

EXPERIMENTAL PROCEDURES

Channel Expression—Human Slo1 (KCNMA1; U11058) and its mutants in the expression vector pCI-neo (Promega), HA-tagged rat TRPM7 (XP_001056331) in pTracer-CMV vector (Invitrogen), and rat SK2 (KCNN2; U69882) in the expression vector pcDNA3 (Invitrogen) were transiently expressed in HEK tsA cells using FuGENE 6 (Roche) as described (29). In some experiments, hSlo1 and β1 (KCNMB1; U38907) in pEGFP-N1 (Clontech) were transfected together with a weight ratio of 1:1. The mutant channels were constructed using a PCR-based mutagenesis method (Agilent), and the sequences were verified (University of Pennsylvania DNA Sequencing Facility).

Electrophysiology and Data Analysis—Ionic currents were recorded using the cell-attached or excised inside-out configuration at room temperature. Patch electrodes (Warner) had a typical initial resistance of 1.5–2.0 megohms. The series resistance, up to 90% of the initial input resistance, was electronically compensated in the macroscopic current measurements. Macroscopic capacitive and leak currents were subtracted using a *P*/6 protocol. The current signal was filtered at 10 kHz through the built-in filter of the patch clamp amplifier (AxoPatch 200A; MDS Analytical Technologies) and digitized at 100 kHz using an ITC-16 AD/DA interface (HEKA). Conductance-voltage (*G-V*) curves were generated from tail currents and fitted with a Boltzmann equation as described (29). The resulting half-activation voltage ($V_{0.5}$) was used to quantify the effect of Zn^{2+} on the channel. Both activation and deactivation time constants were obtained by fitting the currents with a single exponential excluding the initial 180 μs. The results were analyzed as described using IGOR Pro (WaveMetrics) (29). Statistical comparisons between two groups were performed using the unpaired or paired *t* test, as appropriate. Comparison of more than two groups was performed using analysis of variance followed by a Tukey HSD test as implemented in IGOR Pro. Statistical significance was assumed at $p \leq 0.05$, and the data are presented as mean ± S.E. The number of samples in each group is shown in parentheses unless noted otherwise.

Chemicals and Solutions—All chemicals were from Sigma except for 2-aminoethyl methanethiosulfonate hydrobromide (MTSEA; Biotium). TPEN was dissolved in dimethyl sulfoxide and diluted with the internal recording solution to the final concentration of 10 μM. The final concentration of dimethyl sulfoxide (0.02%, v/v) did not affect Slo1 channel currents. For inside-out patch recording, the extracellular solution contained 140 mM KCl, 2 mM $MgCl_2$, 10 mM HEPES, pH 7.2, with *N*-methyl-D-glucamine (NMDG). The intracellular solution contained 140 mM KF, 10 mM HEPES, pH 7.2 or 6.2, with NMDG and a different concentration of $ZnCl_2$ or $ZnSO_4$. The use of KF in the solution limited $[Ca^{2+}] < 20$ nM (30). In the experiments with high concentrations of Ca^{2+}, the intracellular solution did not contain any chelator and the pH was adjusted to 7.2 with NMDG. For the cell-attached patch experiment, the electrode solution contained 140 mM KCl, 2 mM $MgCl_2$ or 2 mM $ZnCl_2$, 10 mM HEPES, pH 7.2, with NMDG. The bath solution contained 130 mM NaCl, 4.0 mM KCl, 2 mM $CaCl_2$, 2 mM $MgCl_2$, 10 mM HEPES, 15 mM glucose, pH 7.4, with NMDG.

RESULTS

Intracellular Zn^{2+} Activates hSlo1 Channels—To observe the effect of cytoplasmic Zn^{2+} on the Slo1 channel while maintaining a very low concentration of Ca^{2+}, we used KF in the internal solution in which most of the contaminating Ca^{2+} precipitated due to the low solubility of CaF_2. In such an internal solution, the free Ca^{2+} concentration has been estimated to be <20 nM (30). Consistently, we found that the activity of the hSlo1 channel remained unaltered when the inside-out patches were transferred from the KF internal solution (see "Experimental Procedures") to the KCl internal solution with 11 mM EGTA in which $[Ca^{2+}]$ is calculated to be <10 nM (WEBMAXC STANDARD; data not shown). In addition, we found that up to 300 μM of Zn^{2+} in the KF solution failed to activate the small-conductance Ca^{2+}-activated channel 2 (SK2), which has higher Ca^{2+} sensitivity than the Slo1 channel (9) (data not shown). These observations together affirmed that $[Ca^{2+}]_i$ was appropriately buffered to a negligible level when Zn^{2+} was added into the KF internal solution.

Addition of Zn^{2+} (0.3–300 μM) quickly and reversibly increased hSlo1 BK currents (Fig. 1, *A* and *C*) in a concentration-dependent manner (Fig. 1*B*). TPEN, a Zn^{2+} chelator with low affinity for Ca^{2+}, fully antagonized the stimulatory effect of the Zn^{2+} addition to the intracellular solution (Fig. 1, *C* and *D*), further confirming that it was Zn^{2+} that increased the hSlo1 current. In contrast, extracellular Zn^{2+}, up to 2 mM, was without any stimulatory effect (see Fig. 6*B*; see also Ref. 31).

The current-enhancing effect of Zn^{2+} was voltage-dependent (Fig. 1*E*) and accompanied by a shift in *G-V* to the hyperpolarized direction without any change in the steepness (Fig. 1*F*). Saturating concentrations of Zn^{2+} (≥100 μM) produced a shift in $V_{0.5}$ of about −75 mV. The Zn^{2+}-dependent shift in *G-V* $V_{0.5}$ had an EC_{50} value of 33.6 ± 12.2 μM and a Hill coefficient of 0.93 ± 0.22 (Fig. 1*G*).

We noticed that high concentrations of Zn^{2+} slightly diminished the peak outward currents at extreme positive voltages (*e.g.* 200 mV in Fig. 1*E*) without decreasing the inward tail current size. This small inhibitory effect, most probably reflecting voltage-dependent block of the channel pore by Zn^{2+} (30), was not investigated any further. In addition to the shift of voltage dependence of activation to the hyperpolarized direction, Zn^{2+} slowed the deactivation kinetics without affecting the activation kinetics (Fig. 1, *H* and *I*).

[3] The abbreviations used are: hSlo1, human Slo1; *G-V*, conductance-voltage; *I-V*, current-voltage; TPEN, *N*,*N*,*N*′*N*′-tetrakis(2-pyridylmethyl)ethylenediamine; MTSEA, 2-aminoethyl methanethiosulfonate hydrobromide; NMDG, *N*-methyl-D-glucamine.

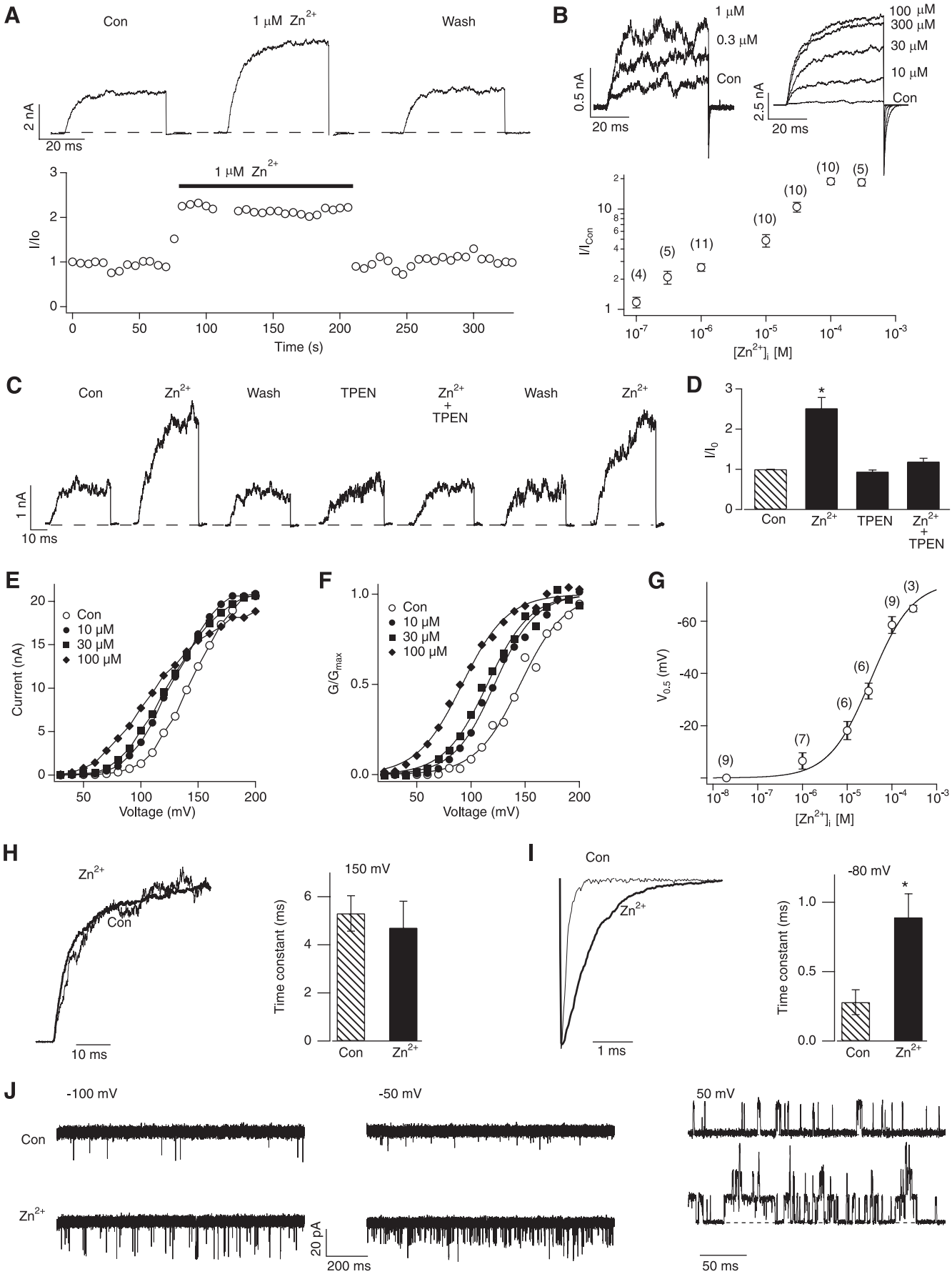
A
Con
1 μM Zn2+
Wash
2 nA
20 ms
1 μM Zn2+
I/Io
Time (s)
B
1 μM
0.3 μM
Con
0.5 nA
20 ms
100 μM
300 μM
30 μM
10 μM
Con
2.5 nA
20 ms
I/ICon
(4)
(5)
(11)
(10)
(10)
(10)
(5)
[Zn2+]i [M]
C
Con
Zn2+
Wash
TPEN
Zn2+ + TPEN
Wash
Zn2+
1 nA
10 ms
D
I/I0
Con
Zn2+
TPEN
Zn2+ + TPEN
E
Con
10 μM
30 μM
100 μM
Current (nA)
Voltage (mV)
F
Con
10 μM
30 μM
100 μM
G/Gmax
Voltage (mV)
G
V0.5 (mV)
(9)
(7)
(6)
(6)
(9)
(3)
[Zn2+]i [M]
H
Zn2+
Con
10 ms
150 mV
Time constant (ms)
Con
Zn2+
I
Con
Zn2+
1 ms
-80 mV
Time constant (ms)
Con
Zn2+
J
-100 mV
-50 mV
Con
Zn2+
20 pA
200 ms
50 mV
50 ms

The stimulatory effect of Zn^{2+} was also observed at the single-channel level. Zn^{2+} drastically increased single-channel open probability in a wide range of voltages, including a physiologically relevant negative voltage (−50 mV) and an extreme negative voltage where the primary voltage sensors of the channel are not activated (Fig. 1*J*). Zn^{2+} had no noticeable effect on the unitary current size (Fig. 1*J*).

Zn^{2+}-dependent Activation of the hSlo1 BK Channel Did Not Require the Conserved Zinc-binding Motifs—Structural studies suggest that histidine and cysteine are the two most frequently used zinc ligands in metalloproteins, in which zinc interacts with the imidazole nitrogen or thiol sulfur in the conserved zinc-binding motifs such as H*XXX*H, and C*XXX*H (*X* represents any amino acid) (2–4, 27, 28, 32). Mutation of either histidine residue in the conserved motif typically disrupts the Zn^{2+} coordination and reduces catalytic activity of metalloenzymes (26, 33). Inspection of the hSlo1 sequence shows that the cytoplasmic domain of the channel contains three putative zinc-binding motifs, ^{464}**H**NKA**H**^{468}, ^{749}**H**ELK**H**^{753}, and ^{612}**C**KAC**H**^{616}, localized in RCK1, RCK2, and the linker region between the two RCK domains, respectively (Fig. 2*A*). To assess the contributions of His and Cys to the Zn^{2+}-induced Slo1 BK channel activation, we utilized diethyl pyrocarbonate, a histidine-modifying reagent (34), and a cysteine-modifying reagent, MTSEA (35). Our results showed that pretreatment of the channel with diethyl pyrocarbonate significantly attenuated the Zn^{2+}-induced activation of the channel, decreasing the $V_{0.5}$ shift to ~50% of that observed in the control group (Fig. 2, *B* and *H*). In contrast, MTSEA failed to alter the Zn^{2+}-induced channel activation (Fig. 2, *C* and *H*). We thus reasoned that the Slo1 protein interacts with Zn^{2+} using histidine residues, possibly in the aforementioned zinc motifs (Fig. 2*A*).

The potential involvement of the histidine residues in the zinc-binding motifs in the channel was further tested by mutation of His^{464}, His^{616}, His^{749}, and His^{753}. A robust stimulatory effect of Zn^{2+}, indistinguishable from that in the wild-type channel, remained in these His-to-Arg mutants (Fig. 2, *D–F*). The mutant channel H616R (29) did not express well enough to record macroscopic currents; however, the mutant retained a Zn^{2+} sensitivity indistinguishable from that of the wild-type channel based on single-channel measurements (Fig. 2*G*). These results collectively indicated that the His residue(s) that coordinate Zn^{2+} are located elsewhere.

Zn^{2+} Is Less Effective at Low pH—The bound Zn^{2+} can be removed from the metalloenzymes in low pH conditions, possibly owing to the protonation of imidazole nitrogens (36). We therefore examined whether intracellular H^+ affected the action of Zn^{2+} on the Slo1 channel. The Zn^{2+}-induced shift in $V_{0.5}$ was indeed significantly reduced in the pH 6.2 internal solution to −25.1 ± 7.1 mV, less than a half of that at pH 7.2 ($p < 0.01$; Fig. 3, *A* and *F*).

Mutation of His^{365} Abolishes the Zn^{2+} Effect—We previously demonstrated that two His residues, His^{365} and His^{394}, in the RCK1 domain serve as the primary H^+ sensors of the hSlo1 channel and mediate pH-dependent activation of the channel (37, 38). The antagonistic effect of low pH on the Zn^{2+}-dependent activation suggests that the same His residues may be required for the Zn^{2+} action. Consistent with this possibility, the double mutation H365R/H394R completely abolished the effect of Zn^{2+} on $V_{0.5}$; the $\Delta V_{0.5}$ value was −2.8 ± 5.1 mV ($p <$ 0.001 compared with the wild-type channel; Fig. 3, *B* and *F*). Of the two His residues, His^{365} clearly plays the most important role, for the single mutation H365R alone eliminated the Zn^{2+} sensitivity ($\Delta V_{0.5} = -5.5 \pm 2.9$ mV; $p < 0.0001$ compared with the wild-type channel; Fig. 3, *C* and *F*). Mutation of His^{365} to neutral alanine (H365A) also completely disrupted the Zn^{2+} sensitivity of the channel (−6.0 ± 3.9 mV; $p < 0.001$ compared with the wild-type channel and $p > 0.5$ compared with H365R) (Fig. 3, *D* and *F*). In contrast, the mutant H394R remained fully Zn^{2+}-sensitive ($\Delta V_{0.5} = -55.2 \pm 1.2$ mV; $p > 0.5$; Fig. 3, *E* and *F*). While both His^{365} and His^{394} in the RCK1 domain are important for pH-dependent activation of the hSlo1 channel (37, 38), only His^{365} is required for the Zn^{2+}-dependent activation of the channel.

Select Acidic Residues in the RCK1 Domain Implicated in the Ca^{2+} Sensitivity Are also Important for the Zn^{2+} Action—His^{365}, required for the Zn^{2+}-dependent activation of the hSlo1 channel (see Fig. 3) also participates in both Ca^{2+}- and H^+-dependent activation of the Slo1 channel such that the stimulatory effect of H^+ is diminished at higher concentrations of Ca^{2+} (37, 38). We hypothesized that Ca^{2+} may also interfere with the Zn^{2+}-dependent activation of the channel. As predicted by this idea, we found that in the presence of 100 μM Ca^{2+}, which is a saturating concentration for the high-affinity Ca^{2+} sensors of the Slo1 channel (39–42), Zn^{2+} failed to alter *G-V* (Fig. 4, *B* and *F*), indicative of a functional competition between Zn^{2+} and Ca^{2+}.

FIGURE 1. **Application of Zn^{2+} to the cytoplasmic side activates hSlo1 channels.** *A*, representative hSlo1 currents at 100 mV without and with 1 μM Zn^{2+} (*top*). The currents were elicited by pulses from 0 to 100 and then to 0 mV. The peak outward current size at 100 mV is plotted as a function time (*bottom*). *B*, representative hSlo1 currents (*top*) and values of normalized currents (I/I_{Con}, *bottom*) at different concentrations of Zn^{2+} at 100 mV. The values of I/I_{Con} were 1.17 ± 0.14, 2.09 ± 0.31, 2.62 ± 0.62, 4.88 ± 0.68, 10.50 ± 1.19, 18.90 ± 1.40, and 18.41 ± 1.52 at 0.1, 0.3, 1, 10, 30, 100, and 300 μM Zn^{2+}, respectively. The currents were elicited by pulses from 0 to 100 and then to −80 mV. *C*, Zn^{2+} reversibly and repeatedly increased hSlo1 channel currents, but 10 μM TPEN abolished the effect of Zn^{2+}. The currents were elicited as in *A*. *D*, fractional increase in the peak current size by Zn^{2+} (10 μM) in the absence and presence of TPEN (10 μM). The currents were elicited as in *C*. *, $p < 0.01$ compared with control group ($n = 3$ in each group). *E*, *I-V* curves of hSlo1 channels in the absence (*open circles*) and presence of 10 μM (*filled circles*), 30 μM (*filled squares*), and 100 μM (*filled diamonds*) Zn^{2+}. *F*, *G-V* curves of hSlo1 channels with different concentrations of Zn^{2+}: 0 μM (no Zn^{2+} added; *open circles*), 10 μM (*filled circles*), 30 μM (*filled squares*), and 100 μM (*filled diamonds*). The steepness of the *G-V* curves with Zn^{2+} was not different to that in the control condition ($p > 0.69$). *G*, $V_{0.5}$ changes by different concentration of Zn^{2+}. The concentration response was fitted by a Hill equation, $\Delta V_{0.5}(x) = \Delta V_{0.5(max)}/[1 + (EC_{50}/x)^n]$ where *n* is the Hill coefficient, *x* is the Zn^{2+} concentration, and $\Delta V_{0.5(max)}$ is the maximal shift in $V_{0.5}$. *H*, representative normalized currents recorded at 150 mV before (*thin trace*) and after (*thick trace*) application of 100 μM Zn^{2+} (*left*). Time constants of activation before and after application of 100 μM Zn^{2+} ($n = 7$ in each group) (*right*). *I*, representative normalized currents recorded at −80 mV after 40-ms pulses of 150 mV in the absence (*thin trace*) and presence (*thick trace*) of 100 μM Zn^{2+} (*left*). Time constants of deactivation before and after application of 100 μM Zn^{2+} ($n = 8$ in each group) (*right*). *, $p < 0.05$ compared with control group. *J*, representative single-channel currents from different patches at −100, −50, and 50 mV before and after application of Zn^{2+}. 10 μM and 100 μM Zn^{2+} were used at positive and negative voltages, respectively. *Con*, control.

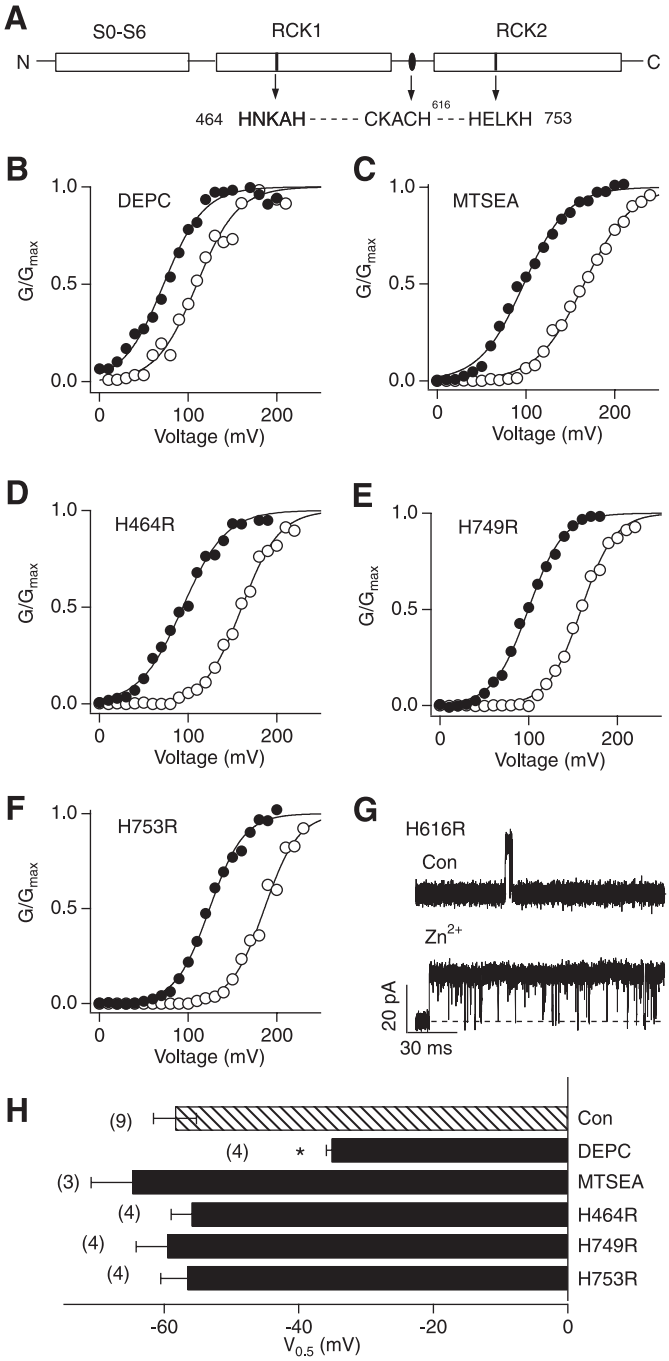

FIGURE 2. **Zn^{2+} remains effective in mutant Slo1 channels with the conserved zinc-binding motifs disrupted.** *A*, a schematic representation of the wild-type hSlo1 channel, showing three potential Zn^{2+}-binding motifs in the RCK1 and RCK2 domains and the linker between of the two domains (*top*). *B* and *C*, representative *G-V* curves before (*open circles*) and after (*filled circles*) application of 100 μM Zn^{2+} following pretreatment with 2 mM diethyl pyrocarbonate for 5 min (*B*) and 1 mM MTSEA for 10 min (*C*). *D–F*, representative *G-V* curves of the His-to-Arg mutant channels indicated in the absence (*open circle*) and presence (*filled circle*) of 100 μM Zn^{2+}. *G*, representative single-channel currents recorded from hSlo1 H616R in the absence (*top*) and presence (*bottom*) of 100 μM Zn^{2+}. The single-channel openings were elicited by pulses to 100 mV from 0 mV. Similar results were observed in another three patches. *H*, changes in $V_{0.5}$ by 100 μM Zn^{2+} in the wild-type channels with and without diethyl pyrocarbonate or MTSEA pretreatment and also in the His-to-Arg mutants. *, $p < 0.001$ compared with the no treatment wild-type group.

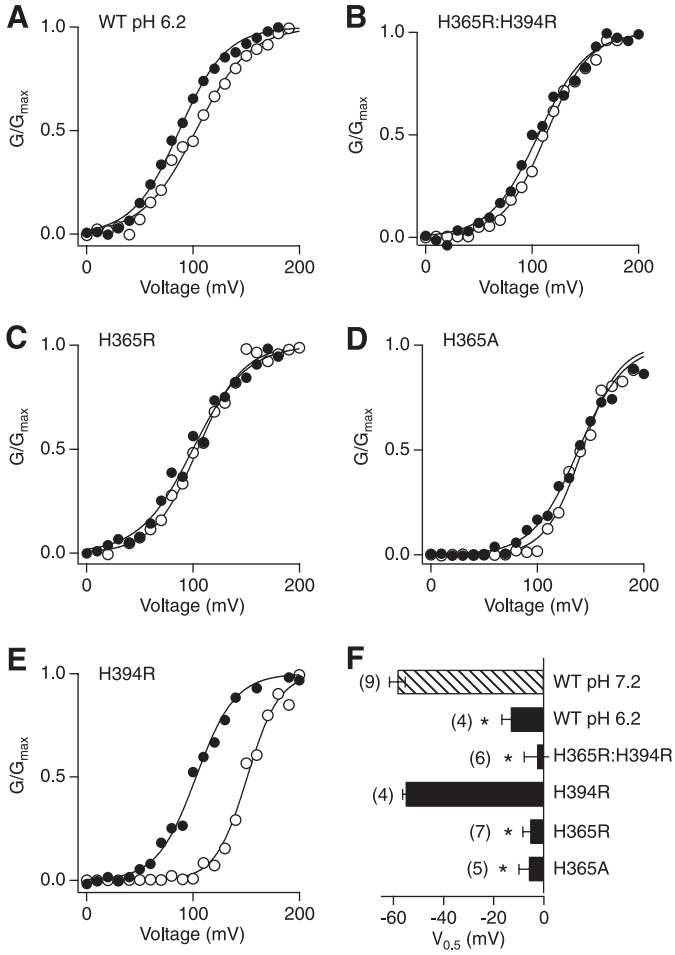

FIGURE 3. **His^{365} in the RCK1 domain is required for Zn^{2+} action.** *A*, *G-V* curves in the wild-type channel at pH 6.2 with (*filled circles*) and without (*open circles*) 100 μM Zn^{2+}. *B–E*, typical *G-V* curves in the His mutants at pH 7.2 before (*open circles*) and after (*filled circles*) application of 100 μM Zn^{2+}. *F*, changes in $V_{0.5}$ in the wild-type channel at pH 7.2 and 6.2 and in the His mutants at pH 7.2. *, $p < 0.001$ compared with the wild-type (*WT*) channel at pH 7.2.

Previous mutagenesis studies suggest the presence of at least three potential divalent cation sensors in each Slo1 subunit (18, 41–43) (Fig. 4*A*); a high-affinity sensor in the RCK1 domain, a high-affinity Ca^{2+} bowl sensor, and a low affinity sensor in the RCK1 domain that also mediates Mg^{2+}-dependent activation of the channel (42). The charge-neutralization mutation D367A in the RCK domain is known to disrupt the high-affinity Ca^{2+}-sensing by the RCK1 domain (41). We found that the mutation significantly decreased the shift in $V_{0.5}$ by 100 μM Zn^{2+} by ~35% to -36.9 ± 5.6 mV ($p < 0.01$ compared with the wild-type channel; Fig. 4, *C* and *F*). The function of the high-affinity Ca^{2+} bowl sensor in the RCK2 domain is disrupted by the deletion mutation Δ884–885 (39). This deletion mutation, however, failed to alter the stimulatory effect of Zn^{2+} on the channel (Fig. 4, *D* and *F*).

The low-affinity divalent cation sensitivity of the Slo1 channel is in part mediated by Glu^{399} in the RCK1 domain (43). The mutation E399A, which impairs the stimulatory action of mM levels of Mg^{2+} on the channel (42, 43), noticeably attenuated the Zn^{2+}-dependent shift in $V_{0.5}$ by ~35% to -37.2 ± 1.8 mV

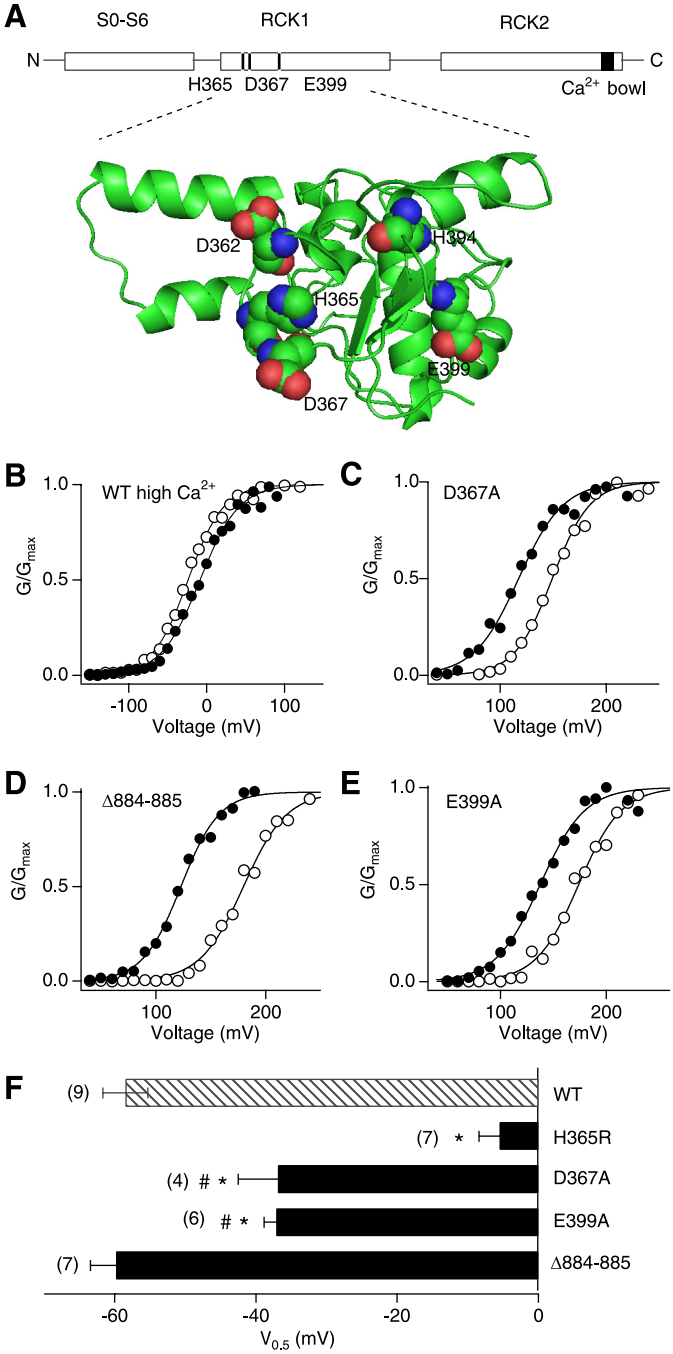

FIGURE 4. **Negatively charged residues in the RCK1 domain contribute to the Zn^{2+}-dependent activation of the Slo1 channel.** *A*, a schematic representation of the potential Zn^{2+}/Ca^{2+} sites in the wild-type hSlo1 channel (*top*) and a homology model of the mouse Slo1 (mSlo1) RCK1 domain (*bottom*) based on the structure of MthK channel (62). The residues required for the effects of Zn^{2+}, Ca^{2+}, and Mg^{2+} are highlighted. The mSlo1 sequence is identical to that of hSlo1 in the RCK1 domain. The images were prepared with MacPyMOL. *B*, a representative *G-V* curve in the wild-type channel in the presence of 200 μM Ca^{2+} alone (*open circles*) and of 200 μM Ca^{2+} and 100 μM Zn^{2+} together (*filled circles*). *C–E*, representative *G-V* curves in the Ca^{2+} sensor mutants in the absence (*open circles*) and presence (*filled circles*) of 100 μM Zn^{2+}. *F*, changes in $V_{0.5}$ caused by 100 μM Zn^{2+} in the wild-type (*WT*) and the mutant channels. The mutation Δ884–885 impairs the Ca^{2+} bowl function (39). *, $p < 0.001$ compared with the wild-type channel and #, $p < 0.01$ compared with the H365R channel.

($p < 0.01$ compared with the wild-type channel; Fig. 4, *E* and *F*). The shifts in $V_{0.5}$ by Zn^{2+} in the D367A and E399A mutants were statistically indistinguishable (Fig. 4*F*).

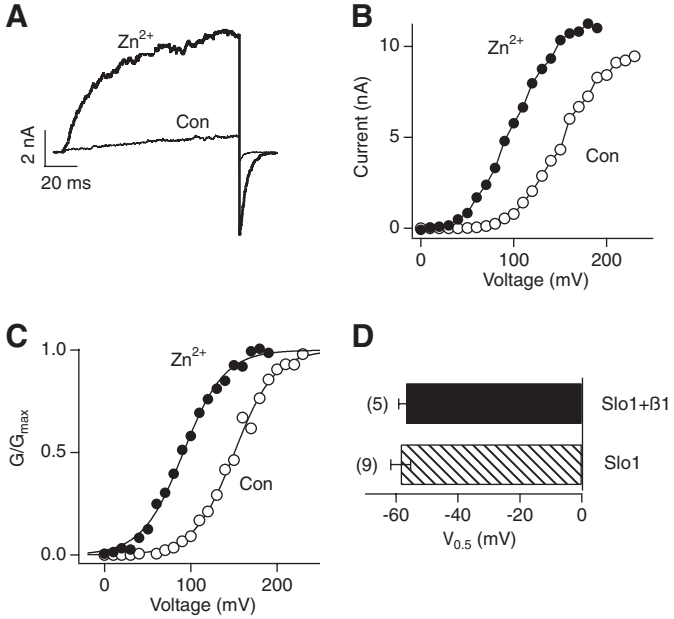

FIGURE 5. **Coexpression of β1 does not alter the effectiveness of Zn^{2+}.** *A*, representative hSlo1+β1 currents at 100 mV before (*thin trace*) and after (*thick trace*) application of 100 μM Zn^{2+}. The currents were elicited by pulses from 0 to 100 and then to −80 mV. *B* and *C*, typical *I-V* curves and *G-V* curves of hSlo1+β1 channels in the absence (*open circles*) and presence (*filled circles*) of 100 μM Zn^{2+}. *D*, changes in $V_{0.5}$ caused by 100 μM Zn^{2+} in Slo1 channel with or without the β1 subunit.

Other transition metals, such as Mn^{2+}, also activate the Slo1 channel (30, 42). We found that the effect of Mn^{2+} was completely disrupted by the mutation E399A but not by the mutation H365A, which eliminates the Zn^{2+} sensitivity (supplemental Fig. S1).

Coexpression of β1 Subunit Does Not Alter the Effect of Zn^{2+}—In addition to the four pore-forming Slo1 subunits, a native BK channel complex may also include auxiliary β subunits in a tissue-dependent manner (44). Heterologous coexpression of the auxiliary subunit β1, predominantly expressed in the cardiovascular system, dramatically increases the overall Ca^{2+} sensitivity and slows both the activation and deactivation kinetics of the channel complex (44). The underlying mechanism is postulated to involve an increase in the Ca^{2+} affinity of the high-affinity Ca^{2+} sensors in the RCK1 domain and the Ca^{2+} bowl in the RCK2 domain (45). Because the stimulatory effect of Zn^{2+} on the Slo1 channel was in part dependent on Asp^{367}, an established component in the high-affinity RCK1 Ca^{2+} sensor (41), we examined whether coexpression of β1 enhanced the effectiveness of Zn^{2+}. Functional coexpression of β1 was verified by the characteristically slower activation and deactivation kinetics. We found that Zn^{2+} remained effective in enhancing the Slo1 current. The shift in $V_{0.5}$ (−56.8 ± 2.4 mV) was indistinguishable from that without coexpression of β1 (Fig. 5; $p > 0.5$).

Extracellular Zn^{2+} Activates Slo1 BK Channel when Coexpressed with TRPM7—Many membrane transport proteins including ion channels mediate translocation of the extracellular Zn^{2+} into intracellular space. Extracellular Zn^{2+} did not affect the Slo1 channel activity; however, it robustly activated the channels when they were coexpressed with TRPM7, a non-

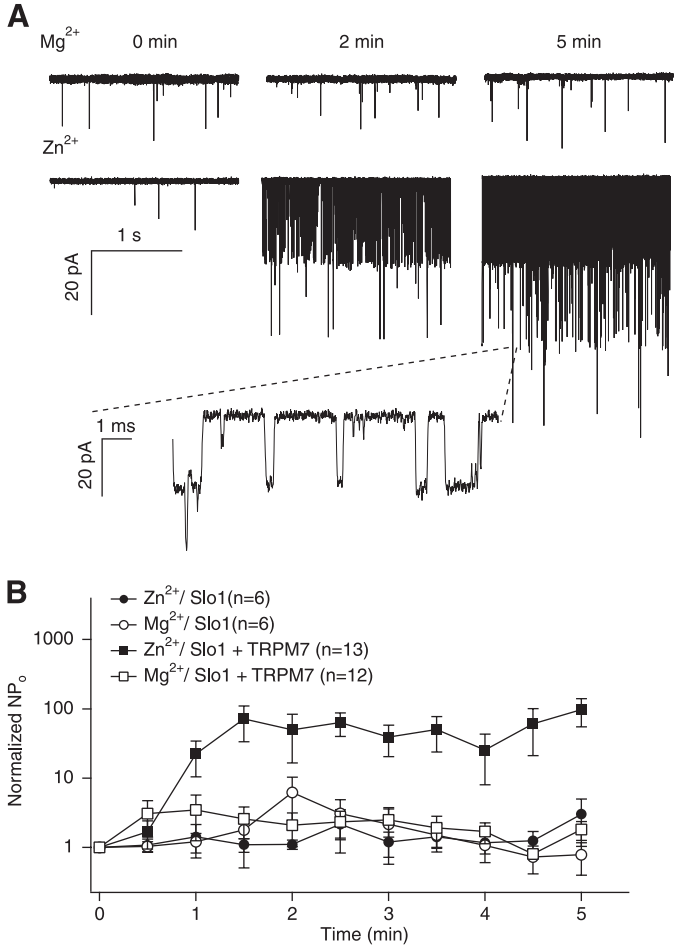

FIGURE 6. **Coexpression with TRPM7 channels facilitates opening of hSlo1 channels.** *A*, representative hSlo1 currents recorded at the time indicated in the presence of extracellular Mg^{2+} (*top*) or Zn^{2+} (*bottom*). Single-channel currents were recorded at −80 mV in the cell attached configuration from cells transfected with hSlo1 and TRPM7. The time 0 min indicates seal formation. Similar results were obtained in 8 of 13 cells. *B*, mean time courses of changes in channel open probability in the presence of extracellular Mg^{2+} (*open symbols*) or Zn^{2+} (*filled symbols*) with hSlo1 channels alone (*circles*) or with hSlo1 and TRPM7 channels together (*squares*). Single channel currents were recorded as in *A*. *N*, number of channels; P_o, open probability.

selective cation channel permeable to Zn^{2+} (46, 47). In contrast, extracellular Mg^{2+} did not alter Slo1 channel open probability (Fig. 6).

DISCUSSION

Zn^{2+} is well known for its structural role in a large number of metalloproteins, including some voltage-gated K^+ channels in which the metal ion mediates tetramerization of the channel proteins (48, 49). As an important intracellular messenger, Zn^{2+} also modulates multiple signaling pathways, but yet only a small number of its direct effectors have been clearly identified (5, 7). Among ion channels, recent studies show that the TRPA1 (transient receptor potential channel A1) (50, 51) and the ATP-sensitive K^+ channel (K_{ATP}) (52) are activated by intracellular Zn^{2+} at nM and μM concentrations, respectively. Our study now adds the Slo1 channel as a new member of the Zn^{2+} signaling cascades. Heterologously expressed Slo1 BK channels are robustly activated by μM levels of intracellular Zn^{2+} in cell-free membrane patches, independently of the auxiliary subunit β1. Moreover, mutation of His^{365} in the RCK1 domain or nearby Asp^{367} or Glu^{399} involved in the Ca^{2+} sensing fully or partially abolished the channel activation by Zn^{2+}.

Our finding that Zn^{2+} activates heterologously expressed Slo1 channels is in contrast with a previous report that Zn^{2+} had no effect on rat skeletal muscle BK channels incorporated in planar lipid bilayers (30). The reason for the apparent discrepancy is not clear. It may be noted that the authors also failed to observe any stimulatory effect of Mg^{2+}, an established activator of Slo1 channels (43, 53) in the same study (30).

The Mechanism of Channel Activation by Zn^{2+}—The functional competition between Zn^{2+} and Ca^{2+} in activation of the Slo1 channel observed in this study is in line with the mutagenesis result that Asp^{367}, essential for the normal high-affinity Ca^{2+} sensing of the channel (41), is also required for Zn^{2+} action. Accordingly, the mechanism of channel activation by Zn^{2+} may be similar to that by Ca^{2+}. Although physical measurements of Ca^{2+} binding to the RCK1 sensor and the Ca^{2+} bowl sensor are preliminary (54–56), conformational changes in an isolated hSlo1 cytoplasmic domain induced by Ca^{2+} have been detected (54). Structural and functional studies of MthK and Slo1 suggest that Ca^{2+}-dependent activation of the Slo1 channel may be accompanied by an expansion of the cytoplasmic domain termed a "gating ring" (22), the mechanical energy of which is further coupled to the channel pore (19, 57). Like Ca^{2+}, Zn^{2+} may induce a similar expansion of the gating ring to promote activation of the channel. However, some differences between the effects of Ca^{2+} and Zn^{2+} exist. The maximal shift in $V_{0.5}$ by Zn^{2+}, about −75 mV, is clearly smaller than that by Ca^{2+}, which can produce a shift of −200 mV at 300 μM (42). One readily discernible reason for the difference is that the Ca^{2+} action is supported by both the sensor in the RCK1 domain and the Ca^{2+} bowl sensor in the RCK2 domain (39, 41, 54, 58). Even in the absence of the Ca^{2+} bowl sensor, 300 μM Ca^{2+} can produce a −125 mV shift (41), still greater than that by Zn^{2+}. The maximal $V_{0.5}$ shift by Zn^{2+} is similar to that caused by H^+, which also works via the RCK1 sensor and functionally competes with Ca^{2+} (37). The smaller shift by H^+ is attributed to weaker allosteric coupling between the gate of the channel and the RCK1 sensor when H^+ is bound as compared with that with Ca^{2+} bound (38). Thus, the coupling strength in the presence of Zn^{2+} may be similarly lower than that with Ca^{2+}. Another difference between the effects of Ca^{2+} and Zn^{2+} relates to Glu^{399} in the RCK1 domain, a critical component in the low-affinity divalent ion sensing of the channel, and its neutralization impairs the channel activation by mM levels of Mg^{2+} (43). Whereas the stimulatory effect of μM levels of Ca^{2+} does not depend on Glu^{399}, the effect of Zn^{2+} is diminished when Glu^{399} is neutralized (Fig. 4). The action of Zn^{2+} is thus influenced by the residues involved in both the high-affinity and low affinity divalent cation sensing mechanism (19). The biophysical mechanism of the channel activation by Zn^{2+} may be similar to that by Ca^{2+} because, unlike effect of Mg^{2+} (59), the Zn^{2+} action remains effective even at negative voltages where the voltage sensors of the channel are not activated. Finally, coexpression with β1 enhances the shift in $V_{0.5}$ by Ca^{2+} but does not alter that by Zn^{2+} (Fig. 5). A similar β1-indepenent effect is

observed with intracellular H^+ (37, 38) further supporting the idea that Zn^{2+} and H^+ may share a similar mechanism in Slo1 channel activation.

Zinc Coordination by Slo1—In many metalloproteins that contain zinc as a stable cofactor, the metal is coordinated by a water molecule and three to four ligands provided by the amino acid residues, typically the side chains of His, Glu, Asp, and Cys (4). Some proteins coordinate zinc using His, Asp, and Glu (4). In Slo1, at least His^{365}, Asp^{367}, and Glu^{399} contribute to the stimulatory effect of Zn^{2+} and His365 is required. The lack of a high-resolution atomic structure of the channel, however, precludes a detailed inference on the zinc coordination geometry. Furthermore, unlike most other zinc-containing proteins, binding of Zn^{2+} to the channel is rapid and readily reversible, and it is not clear how applicable the structural information obtained from the metalloproteins that contain zinc as a stable cofactor may be to the Slo1 protein. Many intracellular EF-hand Ca^{2+}-binding proteins also reversibly bind to Zn^{2+} at concentrations similar to those used to activate Slo1 BK channels (28). Structural studies suggest that Zn^{2+} is often located in close proximity to Ca^{2+} sites and that the two ions reciprocally modulate binding of the other (60, 61), in agreement with our finding that Ca^{2+} and Zn^{2+} competitively activate Slo1 BK channel. The RCK1 domain, which contains the His residue essential for the Zn^{2+} action, was once postulated to contain an EF-hand-like domain (55). However, subsequent structural studies on the prokaryotic channel MthK, which shares a high level of sequence similarity in this area with the Slo1 BK channel, did not support this idea (22, 23). The homology model of Slo1 (Fig. 4*A*) (62) based on the MthK structure clearly shows that Asp^{367} and Glu^{399}, are located in the vicinity of His^{365}, forming a potential ligand binding pocket that accommodates a Ca^{2+}, H^+, or carbon monoxide (37, 63). The requirement for His and the contributions from Asp and Glu in Zn^{2+} activation of the Slo1 channel are in line with the zinc coordination schemes found in metalloproteins such as an *Escherichia coli* rhamnose isomerase (4, 64). We therefore suggest that His^{365}, Asp^{367}, and Glu^{399} in the RCK1 sensor coordinate Zn^{2+}, and the conformational change of the sensor promotes opening of the gate. In TRPA1 channels, which are also activated by intracellular Zn^{2+}, His and Cys residues located some distance away in the primary sequence appear to play a critical role in the Zn^{2+} sensitivity (51).

Physiological and Pathophysiological Implications—Our study demonstrated that human Slo1 BK channels were activated by high nM to μM of intracellular Zn^{2+}. Similar concentrations were also used in Zn^{2+} modulation of other intracellular proteins such as mitochondrial enzymes (65–67) and ion channels (52). For instance, the EC_{50} for activation of recombinant K_{ATP} channels, sulfonylurea receptor (SUR)1/Kir6.2 and SUR2A/Kir6.2 are 1.8 and 60 μM, respectively (52). Such $[Zn^{2+}]_i$ may not be observed physiologically in the bulk intracellular compartment. However, local $[Zn^{2+}]_i$ may reach higher levels near intracellular Zn^{2+} stores or Zn^{2+} permeable channels and it plays important roles in normal neuronal transmission and immune response (5, 7, 68). Interestingly, some Zn^{2+}-permeable ion channels may physically colocalize with Slo1 BK channels, potentially exposing the latter to a locally high level of Zn^{2+} (69). Although quantitative studies of such local Zn^{2+} domains are unavailable, functional analyses of local Ca^{2+} domains suggest that the $[Ca^{2+}]_i$ near Slo1 BK channels can be a few orders of magnitude greater than the mean bulk concentration (9, 69). Thus it is plausible that the local $[Zn^{2+}]_i$ increases transiently to a μM level to activate Slo1 BK channels. Our results (Fig. 6) show that such an increase in $[Zn^{2+}]_i$ could occur through an influx of Zn^{2+} from the extracellular compartments mediated by Zn^{2+}-permeable TRPM7 channels (46, 47, 70). The extracellular concentration of Zn^{2+} in confined compartments such as synaptic clefts may reach several hundred μM (5). Because both TRPM7 and Slo1 BK channels are widely expressed, TRPM7 channels could inject enough Zn^{2+} to activate Slo1 BK channels. Along with TRPA1 (50, 51) and K_{ATP} channels (52), Slo1 BK channels now represent a family of intracellular Zn^{2+}-activated ion channels that could play physiological roles. Increases in $[Zn^{2+}]_i$ may be even greater under some pathological conditions such as brain ischemia/reperfusion and epilepsy (5, 12). For example, in the experimental seizures induced by kainic acid, $[Zn^{2+}]_i$ may increase to hundreds of nM and several μM in hippocampal and cortical neurons, respectively (71, 72). A recent study suggests that the actual increase in $[Zn^{2+}]_i$ during brain ischemia and reperfusion may be significantly more than previously estimated because the divalent cation overload traditionally thought to be from Ca^{2+}, is actually from Zn^{2+} (10). This interpretation and the observation that $[Ca^{2+}]_i$ may reach 30 μM during ischemia (12) together indicate the actual $[Zn^{2+}]_i$ may be in the μM range, sufficient to activate Slo1 BK channels, suggesting that Zn^{2+}-dependent activation of Slo1 BK channels may play a role during cerebral ischemia. The finding that pharmacological activation of BK channels is cell protective during ischemic stroke (24, 25) indicates that the Zn^{2+}-dependent activation of the channel probably represents a compensatory and adaptive response.

In summary, this study demonstrates that hSlo1 BK channels are intracellular Zn^{2+}-activated channels and represent a new effector of intracellular Zn^{2+} signaling. The stimulatory effect of Zn^{2+} requires His, Asp and Glu in the RCK1 domain. As a member of the Zn^{2+}-signaling cascade, Slo1 BK channels may participate in many phenomena mediated by intracellular Zn^{2+}, particularly in some diseases associated with a significant increase in $[Zn^{2+}]_i$.

Acknowledgments—We thank Mark F. Reynolds (Saint Joseph's University, Philadelphia, PA) and Frank T. Horrigan (Baylor College of Medicine, Houston, TX) for discussion and Terry Dean and Yuan Wen for reading of the manuscript.

REFERENCES

1. Sandstead, H. H. (2000) *J. Nutr.* **130,** 347S–349S
2. Vallee, B. L., and Falchuk, K. H. (1993) *Physiol. Rev.* **73,** 79–118
3. Rulísek, L., and Vondrásek, J. (1998) *J. Inorg. Biochem.* **71,** 115–127
4. Auld, D. S. (2001) *Biometals* **14,** 271–313
5. Frederickson, C. J., Koh, J. Y., and Bush, A. I. (2005) *Nat. Rev. Neurosci.* **6,** 449–462
6. Sensi, S. L., Paoletti, P., Bush, A. I., and Sekler, I. (2009) *Nat. Rev. Neurosci.* **10,** 780–791
7. Yamasaki, S., Sakata-Sogawa, K., Hasegawa, A., Suzuki, T., Kabu, K., Sato,

E., Kurosaki, T., Yamashita, S., Tokunaga, M., Nishida, K., and Hirano, T. (2007) *J. Cell Biol.* **177,** 637–645
8. Li, Y., Hough, C. J., Frederickson, C. J., and Sarvey, J. M. (2001) *J. Neurosci.* **21,** 8015–8025
9. Fakler, B., and Adelman, J. P. (2008) *Neuron* **59,** 873–881
10. Stork, C. J., and Li, Y. V. (2006) *J. Neurosci.* **26,** 10430–10437
11. Choi, D. W., and Koh, J. Y. (1998) *Annu. Rev. Neurosci.* **21,** 347–375
12. Lipton, P. (1999) *Physiol. Rev.* **79,** 1431–1568
13. Karagulova, G., Yue, Y., Moreyra, A., Boutjdir, M., and Korichneva, I. (2007) *J. Pharmacol. Exp. Ther.* **321,** 517–525
14. Chanoit, G., Lee, S., Xi, J., Zhu, M., McIntosh, R. A., Mueller, R. A., Norfleet, E. A., and Xu, Z. (2008) *Am. J. Physiol. Heart Circ. Physiol.* **295,** H1227–H1233
15. Lee, S., Chanoit, G., McIntosh, R. A., Zvara, D. A., and Xu, Z. (2009) *Am. J. Physiol. Heart Circ. Physiol.* **297,** H569–575
16. Powell, S. R., Hall, D., Aiuto, L., Wapnir, R. A., Teichberg, S., and Tortolani, A. J. (1994) *Am. J. Physiol.* **266,** H2497–2507
17. Salkoff, L., Butler, A., Ferreira, G., Santi, C., and Wei, A. (2006) *Nat. Rev. Neurosci.* **7,** 921–931
18. Magleby, K. L. (2003) *J. Gen. Physiol.* **121,** 81–96
19. Cui, J., Yang, H., and Lee, U. S. (2009) *Cell Mol. Life Sci.* **66,** 852–875
20. Adelman, J. P., Shen, K. Z., Kavanaugh, M. P., Warren, R. A., Wu, Y. N., Lagrutta, A., Bond, C. T., and North, R. A. (1992) *Neuron* **9,** 209–216
21. Meera, P., Wallner, M., Song, M., and Toro, L. (1997) *Proc. Natl. Acad. Sci. U.S.A.* **94,** 14066–14071
22. Jiang, Y., Lee, A., Chen, J., Cadene, M., Chait, B. T., and MacKinnon, R. (2002) *Nature* **417,** 515–522
23. Jiang, Y., Pico, A., Cadene, M., Chait, B. T., and MacKinnon, R. (2001) *Neuron* **29,** 593–601
24. Gribkoff, V. K., Starrett, J. E., Jr., Dworetzky, S. I., Hewawasam, P., Boissard, C. G., Cook, D. A., Frantz, S. W., Heman, K., Hibbard, J. R., Huston, K., Johnson, G., Krishnan, B. S., Kinney, G. G., Lombardo, L. A., Meanwell, N. A., Molinoff, P. B., Myers, R. A., Moon, S. L., Ortiz, A., Pajor, L., Pieschl, R. L., Post-Munson, D. J., Signor, L. J., Srinivas, N., Taber, M. T., Thalody, G., Trojnacki, J. T., Wiener, H., Yeleswaram, K., and Yeola, S. W. (2001) *Nat. Med.* **7,** 471–477
25. Xu, W., Liu, Y., Wang, S., McDonald, T., Van Eyk, J. E., Sidor, A., and O'Rourke, B. (2002) *Science* **298,** 1029–1033
26. Rawlings, N. D., and Barrett, A. J. (1995) *Methods Enzymol.* **248,** 183–228
27. Sankaranarayanan, R., Dock-Bregeon, A. C., Romby, P., Caillet, J., Springer, M., Rees, B., Ehresmann, C., Ehresmann, B., and Moras, D. (1999) *Cell* **97,** 371–381
28. Korndörfer, I. P., Brueckner, F., and Skerra, A. (2007) *J. Mol. Biol.* **370,** 887–898
29. Tang, X. D., Xu, R., Reynolds, M. F., Garcia, M. L., Heinemann, S. H., and Hoshi, T. (2003) *Nature* **425,** 531–535
30. Oberhauser, A., Alvarez, O., and Latorre, R. (1988) *J. Gen. Physiol.* **92,** 67–86
31. Ma, Z., Wong, K. Y., and Horrigan, F. T. (2008) *J. Gen. Physiol.* **131,** 483–502
32. Volbeda, A., Fontecilla-Camps, J. C., and Frey, M. (1996) *Curr. Opin. Struct. Biol.* **6,** 804–812
33. McGwire, B. S., and Chang, K. P. (1996) *J. Biol. Chem.* **271,** 7903–7909
34. Miles, E. W. (1977) *Methods Enzymol.* **47,** 431–442
35. Karlin, A., and Akabas, M. H. (1998) *Methods Enzymol.* **293,** 123–145
36. Pantoliano, M. W., Valentine, J. S., Burger, A. R., and Lippard, S. J. (1982) *J. Inorg. Biochem.* **17,** 325–341
37. Hou, S., Xu, R., Heinemann, S. H., and Hoshi, T. (2008) *Nat. Struct. Mol. Biol.* **15,** 403–410
38. Hou, S., Horrigan, F. T., Xu, R., Heinemann, S. H., and Hoshi, T. (2009) *Channels* **3,** 249–258
39. Schreiber, M., and Salkoff, L. (1997) *Biophys. J.* **73,** 1355–1363
40. Bao, L., Rapin, A. M., Holmstrand, E. C., and Cox, D. H. (2002) *J. Gen. Physiol.* **120,** 173–189
41. Xia, X. M., Zeng, X., and Lingle, C. J. (2002) *Nature* **418,** 880–884
42. Zeng, X. H., Xia, X. M., and Lingle, C. J. (2005) *J. Gen. Physiol.* **125,** 273–286
43. Shi, J., Krishnamoorthy, G., Yang, Y., Hu, L., Chaturvedi, N., Harilal, D., Qin, J., and Cui, J. (2002) *Nature* **418,** 876–880
44. Torres, Y. P., Morera, F. J., Carvacho, I., and Latorre, R. (2007) *J. Biol. Chem.* **282,** 24485–24489
45. Sweet, T. B., and Cox, D. H. (2009) *J. Gen. Physiol.* **133,** 139–150
46. Runnels, L. W., Yue, L., and Clapham, D. E. (2001) *Science* **291,** 1043–1047
47. Monteilh-Zoller, M. K., Hermosura, M. C., Nadler, M. J., Scharenberg, A. M., Penner, R., and Fleig, A. (2003) *J. Gen. Physiol.* **121,** 49–60
48. Bixby, K. A., Nanao, M. H., Shen, N. V., Kreusch, A., Bellamy, H., Pfaffinger, P. J., and Choe, S. (1999) *Nat. Struct. Biol.* **6,** 38–43
49. Strang, C., Kunjilwar, K., DeRubeis, D., Peterson, D., and Pfaffinger, P. J. (2003) *J. Biol. Chem.* **278,** 31361–31371
50. Andersson, D. A., Gentry, C., Moss, S., and Bevan, S. (2009) *Proc. Natl. Acad. Sci. U.S.A.* **106,** 8374–8379
51. Hu, H., Bandell, M., Petrus, M. J., Zhu, M. X., and Patapoutian, A. (2009) *Nat. Chem. Biol.* **5,** 183–190
52. Prost, A. L., Bloc, A., Hussy, N., Derand, R., and Vivaudou, M. (2004) *J. Physiol.* **559,** 157–167
53. Shi, J., and Cui, J. (2001) *J. Gen. Physiol.* **118,** 589–606
54. Yusifov, T., Savalli, N., Gandhi, C. S., Ottolia, M., and Olcese, R. (2008) *Proc. Natl. Acad. Sci. U.S.A.* **105,** 376–381
55. Braun, A. P., and Sy, L. (2001) *J. Physiol.* **533,** 681–695
56. Bao, L., Kaldany, C., Holmstrand, E. C., and Cox, D. H. (2004) *J. Gen. Physiol.* **123,** 475–489
57. Niu, X., Qian, X., and Magleby, K. L. (2004) *Neuron* **42,** 745–756
58. Qian, X., Niu, X., and Magleby, K. L. (2006) *J. Gen. Physiol.* **128,** 389–404
59. Horrigan, F. T., Cui, J., and Aldrich, R. W. (1999) *J. Gen. Physiol.* **114,** 277–304
60. Ostendorp, T., Heizmann, C. W., Kroneck, P. M., and Fritz, G. (2005) *Acta Crystallogr. Sect. F. Struct. Biol. Cryst. Commun.* **61,** 673–675
61. Koch, M., Bhattacharya, S., Kehl, T., Gimona, M., Vasák, M., Chazin, W., Heizmann, C. W., Kroneck, P. M., and Fritz, G. (2007) *Biochim. Biophys. Acta* **1773,** 457–470
62. Latorre, R., and Brauchi, S. (2006) *Biol. Res.* **39,** 385–401
63. Hou, S., Xu, R., Heinemann, S. H., and Hoshi, T. (2008) *Proc. Natl. Acad. Sci. U.S.A.* **105,** 4039–4043
64. Korndörfer, I. P., Fessner, W. D., and Matthews, B. W. (2000) *J. Mol. Biol.* **300,** 917–933
65. Mills, D. A., Schmidt, B., Hiser, C., Westley, E., and Ferguson-Miller, S. (2002) *J. Biol. Chem.* **277,** 14894–14901
66. Link, T. A., and von Jagow, G. (1995) *J. Biol. Chem.* **270,** 25001–25006
67. Sharpley, M. S., and Hirst, J. (2006) *J. Biol. Chem.* **281,** 34803–34809
68. Permyakov, E. (2009) *Metalloproteomics*, 1st Ed., pp. 283–338, John Wiley & Sons, Inc., Hoboken, NJ
69. Berkefeld, H., Sailer, C. A., Bildl, W., Rohde, V., Thumfart, J. O., Eble, S., Klugbauer, N., Reisinger, E., Bischofberger, J., Oliver, D., Knaus, H. G., Schulte, U., and Fakler, B. (2006) *Science* **314,** 615–620
70. Fonfria, E., Murdock, P. R., Cusdin, F. S., Benham, C. D., Kelsell, R. E., and McNulty, S. (2006) *J. Recept. Signal Transduct. Res.* **26,** 159–178
71. Côté, A., Chiasson, M., Peralta, M. R., 3rd, Lafortune, K., Pellegrini, L., and Tóth, K. (2005) *J. Physiol.* **566,** 821–837
72. Sensi, S. L., Yin, H. Z., Carriedo, S. G., Rao, S. S., and Weiss, J. H. (1999) *Proc. Natl. Acad. Sci. U.S.A.* **96,** 2414–2419